JOURNAL OF MAGNETIC RESONANCE **126,** 110–119 (1997)
ARTICLE NO. MN971157

# ''*Kin*'' HEHAHA Sequences, Heteronuclear Hartmann–Hahn Transfer with Different Bandwidths for Spins I and S

Teresa Carlomagno,* Burkhard Luy, and Steffen J. Glaser†

*Institute of Organic Chemistry, University of Frankfurt, Marie-Curie Strasse 11, D-60439 Frankfurt, Germany*

Received December 3, 1996

**A new class of heteronuclear Hartmann–Hahn experiments that is based on the simultaneous irradiation of two different multiple-pulse sequences is introduced. For these ''*kin*'' HEHAHA sequences, the scaling properties of the effective heteronuclear coupling constants are analyzed. Four *kin* sequences are presented with a ratio of the active bandwidths $\Delta\nu_I/\Delta\nu_S$ ranging between 1/2 and 1/10. The offset dependence of the polarization-transfer efficiency is examined experimentally and with the help of numerical simulations.** © 1997 Academic Press

## INTRODUCTION

Heteronuclear Hartmann–Hahn transfer (HEHAHA) constitutes an important building block in high-resolution multidimensional NMR experiments (*1–5*). The use of HEHAHA mixing sequences for the transfer of magnetization between two scalar-coupled spins is often more efficient than the use of INEPT-type transfer steps because of their better tolerance of RF inhomogeneity (*6*) and of exchange effects (*7*). HEHAHA polarization transfer relying on large one-bond coupling constants, such as $^1J(^1\mathrm{H}, ^{13}\mathrm{C})$, $^1J(^1\mathrm{H}, ^{15}\mathrm{N})$, or $^1J(^1\mathrm{H}, ^{31}\mathrm{P})$, has been extensively applied in multidimensional NMR experiments of biomolecules (*5, 8*). So far, all HEHAHA mixing experiments have been based on the simultaneous irradiation of two identical multiple-pulse sequences $P_I$ and $P_S$ with the same RF amplitudes $\gamma_I B_{1I}(t) = \gamma_S B_{1S}(t)$ at the resonance frequencies of the heteronuclear spins I and S that are involved in the transfer. Whereas this approach is certainly the most direct way to fulfill the Hartmann–Hahn condition and to achieve the maximum transfer rate, it has two important limitations. First, the use of the same multiple-pulse sequence ($P_I = P_S$) for both nuclei implies that the active bandwidths $\Delta\nu_I$ and $\Delta\nu_S$ are also identical, i.e., $\Delta\nu_I/\Delta\nu_S = 1$. This can be of disadvantage in applications in which selectivity is required for one of the two spins (e.g., for spin I), whereas a large frequency range is to be covered for the second spin (S) (*9*). The second limitation regards RF power requirements. In practice, the offset ranges of the two spin species I and S can be very different; for example, in $^1\mathrm{H}-^{31}\mathrm{P}$ HEHAHA experiments of DNA samples (*10, 11*), the offset range $\Delta\nu$ of the protons is a factor of eight larger than the offset range of the $^{31}$P spins. As the active bandwidth of a given multiple-pulse sequence is in general approximately proportional to the RF amplitude $\gamma B_1$, the condition $\gamma_I B_{1I}(t) = \gamma_S B_{1S}(t)$ implies that the total RF power is dictated entirely by the spin species with the largest offset range, regardless of how small the offset range of the other spin species may be.

In this paper we propose a new class of heteronuclear Hartmann–Hahn experiments that are based on the irradiation of *different* multiple-pulse sequences $P_I \neq P_S$ at the resonance frequencies of spins I and S. These sequences must be *related,* in order to preserve the coupling between the two spins, but they can have enough dissimilarities to effect coherence transfer over different bandwidths (i.e., $\Delta\nu_I/\Delta\nu_S \neq 1$) and perhaps also to require nonidentical average RF powers. For brevity, we will refer to this new class of experiments as ''*kin*'' HEHAHA sequences, whereas conventional HEHAHA experiments with *identical* multiple-pulse sequences will be termed ''*twin*'' sequences. The three most important potential problems for the development of efficient *kin* HEHAHA sequences are related to the scaling of the effective heteronuclear coupling constant $J_{IS}^{eff}$, to the match of the Hartmann–Hahn condition, and to their design.

As the rate of HEHAHA transfer is determined by the effective coupling constant, $J_{IS}^{eff}$ should be as large as possible. The reduction in $J_{IS}^{eff}$ is minimal in planar *twin* HEHAHA experiments, where an effective coupling tensor of the form $H_p = J_{IS}^{eff}(I_y S_y + S_z I_z)$ is created (*4, 5*) and the maximum possible effective coupling constant $J_{IS}^{eff}$ is given by $J_{IS}/2$. The application of different multiple-pulse sequences to spins I and S invariably results in a further reduction of the effective coupling constant, i.e., $J_{IS}^{eff} < J_{IS}/2$ for *kin* HEHAHA sequences. However, if the additional scaling of $J_{IS}^{eff}$

* On leave from Institute of Chemistry, University of Naples Federico II, Via Mezzocannone, 4 I-80134 Naples, Italy.
† To whom correspondence should be addressed.



1090-7807/97 $25.00

is only moderate, this disadvantage may be more than compensated by the increased flexibility that is offered by *kin* sequences.

A second possible point of concern is related to the Hartmann–Hahn condition (*1, 5*) which must be fulfilled for efficient HEHAHA transfer. In fact, if continuous-wave irradiation is used, the Hartmann–Hahn condition ($\gamma_I B_{1I} = \gamma_S B_{1S}$) implies the use of *twin*-type RF irradiation. However, in experiments based on multiple-pulse sequences, it is not necessary that the condition $\gamma_I B_{1I}(t) = \gamma_S B_{1S}(t)$ be fulfilled during the entire multiple-pulse sequence. In this case, the Hartmann–Hahn condition only requires the match of the *effective* fields $B_I^{eff}$ and $B_S^{eff}$ (*12, 13*) that are experienced by spins I and S, respectively, i.e., $\gamma_I B_I^{eff} = \gamma_S B_S^{eff}$ (*5*). This condition can also be fulfilled by *kin* HEHAHA sequences.

The lack of efficient tools for the design of *kin* HEHAHA sequences was probably the most important problem for their development in the past. In fact, most heteronuclear Hartmann–Hahn sequences that are currently in use were simply derived from well-known heteronuclear decoupling sequences. Examples are CW irradiation (*1*), WALTZ-16 (*14–17*), and DIPSI-2 (*4, 16*). For heteronuclear decoupling, a given multiple-pulse sequence is irradiated only at the resonance frequency of a single nuclear spin species. In HEHAHA experiments, this sequence is irradiated simultaneously at the resonance frequencies of spins I and S, since the conditions for efficient heteronuclear decoupling and the Hartmann–Hahn condition are related (*5, 18, 19*). Obviously, this simple approach can only yield HEHAHA sequences of the *twin* type. However, recently, several new *twin*-type HEHAHA sequences were developed *de novo*, based on numerical optimizations (*20, 21*), and the established methods for the computer-aided development of multiple-pulse sequences can also be applied to the design of *kin* HEHAHA sequences. In order to explore the potential of these experiments, we attempted to design *kin* HEHAHA sequences where the active bandwidth $\Delta\nu_S$ is up to a factor of ten larger than the active bandwidth $\Delta\nu_I$.

## THEORY

For efficient heteronuclear Hartmann–Hahn transfer of *x* magnetization, an ideal effective Hamiltonian of the form

$$\mathcal{H}_{ideal} = 2\pi J_{IS}^{eff}\{(I_y S_y + I_z S_z)\cos\phi + (I_z S_y - I_y S_z)\sin\phi\} \quad [1]$$

is desired (*5*), where the effective coupling constant $J_{IS}^{eff}$ approaches $J_{IS}/2$ and $\phi$ is an arbitrary zero-quantum phase (*5, 22*). The free evolution Hamiltonian $\mathcal{H}_0$ of the heteronuclear spin system is given by

$$\mathcal{H}_0 = 2\pi\{\nu_I I_z + \nu_S S_z + J_{IS} I_z S_z\}, \quad [2]$$

where $\nu_I$ and $\nu_S$ are the offsets of spins I and S in the doubly rotating frame and $J_{IS}$ is the heteronuclear coupling constant. During an RF pulse, the additional RF term is given by

$$\mathcal{H}_{RF}(t) = 2\pi\nu_{1I}(t)\{I_x\cos\varphi_I(t) + I_y\sin\varphi_I(t)\} + 2\pi\nu_{1S}(t)\{S_x\cos\varphi_S(t) + S_y\sin\varphi_S(t)\}, \quad [3]$$

where the Rabi frequencies $\nu_{1I}(t) = \gamma_I B_{1I}/2\pi$ and $\nu_{1S}(t) = \gamma_S B_{1S}/2\pi$ represent the amplitudes of the two RF fields that are applied at the frequencies of spins I and S, respectively.

In the following, we focus on sequences with constant and equal RF amplitudes for the two spin species, i.e., $\nu_{1I}(t) = \nu_{1S}(t) = \nu_1$. This restriction is imposed for the sake of simplicity and in order to limit the required computation time for the optimization of *kin* sequences. The study of *kin* sequences with unequal RF fields will be the subject of future investigations. In addition, the phases $\varphi_I(t)$ and $\varphi_S(t)$ are restricted to be 0 or $\pi$, in order to minimize the scaling of the effective coupling constant $J_{IS}^{eff}$ (*4, 5*) and for simplicity. Under these conditions, the RF term of the Hamiltonian can be expressed in the form

$$\mathcal{H}_{RF}(t) = \mathcal{H}_{RF,\Sigma}(t) + \mathcal{H}_{RF,\Delta}(t) \quad [4]$$

with

$$\mathcal{H}_{RF,\Sigma}(t) = 2\pi\nu_1(I_x + S_x)\cos\varphi_I(t) \quad [5]$$

and

$$\mathcal{H}_{RF,\Delta}(t) = 2\pi\nu_1 S_x[\cos\varphi_S(t) - \cos\varphi_I(t)]. \quad [6]$$

This partitioning of $\mathcal{H}_{RF}$ into the two commuting parts $\mathcal{H}_{RF,\Sigma}(t)$ and $\mathcal{H}_{RF,\Delta}(t)$ is convenient for the analysis of the characteristic scaling properties of the effective coupling constant $J_{IS}^{eff}$ during a *kin* HEHAHA sequence. The term $\mathcal{H}_{RF,\Sigma}(t)$ corresponds to the RF term of a conventional *twin* HEHAHA sequence that results if the spin I part $P_I$ of a given *kin* sequence is applied both to the I and to the S spins. If different sequences $P_I$ and $P_S$ are applied in *kin* HEHAHA experiments, the additional term $\mathcal{H}_{RF,\Delta}(t)$ arises, which here is nonzero only during time intervals where the RF phases of the sequences $P_I$ and $P_S$ are different. For the analysis, the following sequential transformations into two different toggling frames are of interest. In the first step, the Hamiltonian $\mathcal{H}(t) = \mathcal{H}_0 + \mathcal{H}_{RF}(t)$ is transformed into the toggling frame defined by $\mathcal{H}_{RF,\Sigma}(t)$ alone, where it has the form $\tilde{\mathcal{H}}(t) = \tilde{\mathcal{H}}_0(t) + \tilde{\mathcal{H}}_{RF}(t)$ with

$$\tilde{\mathcal{H}}_0(t) = U^\dagger(t)\mathcal{H}_0U(t), \quad [7]$$

$$\tilde{\mathcal{H}}_{RF}(t) = U^\dagger(t)\mathcal{H}_{RF}(t)U(t) = \mathcal{H}_{RF,\Delta}(t), \quad [8]$$

and

$$U(t) = T\exp\{-i\int_0^t \mathcal{H}_{RF,\Sigma}(t')dt'\}. \quad [9]$$

$T$ is the Dyson time-ordering operator (*23*, *24*). In the second step, $\tilde{\mathcal{H}}(t)$ is transformed into the toggling frame defined by $\tilde{\mathcal{H}}_{RF}(t) = \mathcal{H}_{RF,\Delta}(t)$, where it is reduced to

$$\tilde{\mathcal{H}}'(t) = \tilde{\mathcal{H}}'_0(t) = U'^\dagger(t)\tilde{\mathcal{H}}_0(t)U'(t) \quad [10]$$

with

$$U'(t) = T\exp\{-i\int_0^t \mathcal{H}_{RF,\Delta}(t')dt'\}. \quad [11]$$

In the following discussion, we assume that both $U(t)$ and $U'(t)$ are cyclic, i.e., $U(\tau_c) = U'(\tau_c) = \mathbf{1}$. Suppose, the *twin* sequence defined by $\mathcal{H}_{RF,\Sigma}$ represents a well-designed conventional heteronuclear Hartmann–Hahn sequence which creates a planar average free-evolution Hamiltonian

$$\bar{\tilde{\mathcal{H}}}_0 = \frac{1}{\tau_c}\int_0^{\tau_c}\tilde{\mathcal{H}}_0(t)dt \quad [12]$$

of the form

$$\mathcal{H}_P = 2\pi\bar{J}_{IS,twin}(I_yS_y + I_zS_z) \quad [13]$$

with an average coupling constant $\bar{J}_{IS,twin} \leqslant J_{IS}/2$. Now we are in a position to analyze the effects of applying *different* pulse sequences $P_I$ and $P_S$, where $\mathcal{H}_{RF,\Delta}(t) \neq 0$. In the toggling frame defined by $\tilde{\mathcal{H}}_{RF}(t) = \mathcal{H}_{RF,\Delta}(t)$, the planar Hamiltonian $\mathcal{H}_P$ is time-dependent and has the form

$$\begin{aligned}\tilde{\mathcal{H}}'_P(t) &= U'^\dagger(t)\mathcal{H}_PU'(t)\\ &= 2\pi\bar{J}_{IS,twin}\{(I_yS_y + I_zS_z)\cos\Delta\alpha(t)\\ &\quad + (I_zS_y - I_yS_z)\sin\Delta\alpha(t)\},\end{aligned} \quad [14]$$

where

$$\Delta\alpha(t) = 2\pi\nu_1\int_0^t[\cos\varphi_S(t') - \cos\varphi_I(t')]dt' \quad [15]$$

is the angle between the individual toggling frames defined by the sequences $P_I$ and $P_S$. Whereas for *twin* sequences $\Delta\alpha(t) = 0$ for $0 \leqslant t \leqslant \tau_c$, this angle is in general nonzero for *kin* HEHAHA sequences. The average Hamiltonian

$$\bar{\tilde{\mathcal{H}}}'_P = \frac{1}{\tau_c}\int_0^{\tau_c}\tilde{\mathcal{H}}'_P(t)dt \quad [16]$$

**TABLE 1**
**Pulse Sequence Parameters**

| Sequence: | TC-2 | | TC-3 | | TC-5 | | TC-10 | |
|---|---|---|---|---|---|---|---|---|
| Spin: | I | S | I | S | I | S | I | S |
| $\Delta\nu$ [kHz] | 2.0 | 4.0 | 1.3 | 4.0 | 0.8 | 4.0 | 0.4 | 4.0 |
| $\alpha_1$ | $128.7^\circ_x$ | $140.1^\circ_x$ | $2.2^\circ_x$ | $7.2^\circ_x$ | $230.0^\circ_x$ | $241.3^\circ_x$ | $158.0^\circ_x$ | $154.8^\circ_x$ |
| $\alpha_2$ | $212.8^\circ_{-x}$ | $249.0^\circ_{-x}$ | $242.2^\circ_{-x}$ | $238.9^\circ_{-x}$ | $65.8^\circ_{-x}$ | $62.2^\circ_{-x}$ | $210.3^\circ_{-x}$ | $268.7^\circ_{-x}$ |
| $\alpha_3$ | $78.1^\circ_x$ | $84.8^\circ_x$ | $116.2^\circ_x$ | $287.3^\circ_x$ | $82.4^\circ_x$ | $240.1^\circ_x$ | $72.7^\circ_x$ | $101.3^\circ_x$ |
| $\alpha_4$ | $241.2^\circ_{-x}$ | $196.9^\circ_{-x}$ | $243.0^\circ_{-x}$ | $82.0^\circ_{-x}$ | $317.1^\circ_{-x}$ | $150.0^\circ_{-x}$ | $292.8^\circ_{-x}$ | $213.0^\circ_{-x}$ |
| $\alpha_5$ | $396.5^\circ_x$ | $386.5^\circ_x$ | $190.3^\circ_x$ | $178.5^\circ_x$ | $283.9^\circ_x$ | $285.6^\circ_x$ | $383.4^\circ_x$ | $379.4^\circ_x$ |
| $\alpha(\tau_R)$ | 149.3° | 165.5° | −176.5° | 152.1° | 213.4° | 554.8° | 111.0° | 153.8° |
| $\Delta\alpha(\tau_R)$ | 16.2° | | 328.6° | | 341.4° | | 42.8° | |
| $\bar{c}^R_{\Delta\alpha}$ | 0.90 | | 0.74 | | 0.78 | | 0.75 | |
| $\bar{s}^R_{\Delta\alpha}$ | 0.23 | | −0.06 | | −0.12 | | 0.28 | |
| $\lambda_{kin}$ | 0.91 | | 0.70 | | 0.78 | | 0.74 | |
| $\nu_1$ [kHz] | 7.97 | | 4.62 | | 7.88 | | 7.23 | |
| $\tau_c = 4\tau_R$ [ms] | 1.47 | | 1.91 | | 1.38 | | 1.72 | |

*Note.* The ''*kin*'' HEHAHA sequences TC-2, TC-3, TC-5, and TC-10 with active offset ratios $\Delta\nu_I/\Delta\nu_S$ of 1/2, 1/3, 1/5, and 1/10 are based on composite pulses $R_I$ and $R_S$ that consist of five hard pulses [$R_I = \alpha_1(I), \alpha_2(I), \alpha_3(I), \alpha_4(I), \alpha_5(I)$ and $R_S = \alpha_1(S), \alpha_2(S), \alpha_3(S), \alpha_4(S), \alpha_5(S)$]. The composite pulses of duration $\tau_R$ are expanded in an MLEV-4 cycle (*25*) with the cycle time $\tau_c = 4\tau_R$.

has the form

$$\bar{\bar{\mathcal{H}}}'_{\mathrm{P}} = 2\pi \bar{J}_{\mathrm{IS},twin}\{\bar{c}_{\Delta\alpha}(I_yS_y + I_zS_z) + \bar{s}_{\Delta\alpha}(I_zS_y - I_yS_z)\} \quad [17]$$

with the coefficients

$$\bar{c}_{\Delta\alpha} = \frac{1}{\tau_c}\int_0^{\tau_c} \cos\,\Delta\alpha(t)dt \quad [18]$$

and

$$\bar{s}_{\Delta\alpha} = \frac{1}{\tau_c}\int_0^{\tau_c} \sin\,\Delta\alpha(t)dt. \quad [19]$$

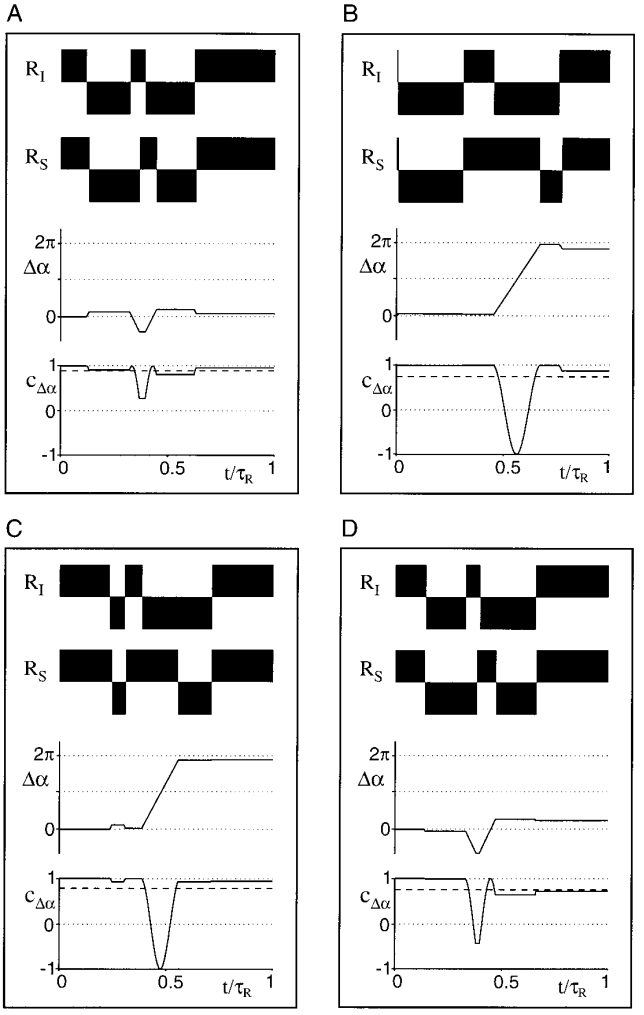


**FIG. 1.** For $0 \leqslant t \leqslant \tau_R = \tau_c/4$, the composite pulses $R_I$ and $R_S$ are shown for the TC-2 (A), TC-3 (B) TC-5 (C), and TC-10 (D) ''*kin*'' HEHAHA sequences (cf. Table 1). Pulses with RF phases $x$ or $-x$ are shown with positive and negative amplitudes, respectively. In addition, the angles $\Delta\alpha(t)$, the cosine $c_{\Delta\alpha}(t) = \cos[\Delta\alpha(t)]$ (solid line), and $\bar{c}^R_{\Delta\alpha}$ (dashed line, cf. Eq. [24]) are shown.

The expressions for the coefficients $\bar{c}_{\Delta\alpha}$ and $\bar{s}_{\Delta\alpha}$ can be further simplified, if the sequences $P_I$ and $P_S$ consist of composite pulses $R_I$ and $R_S$ of equal duration $\tau_{R,I} = \tau_{R,S} = \tau_R$, which are expanded in a cycle or supercycle scheme, such as MLEV-4 (*25*). Here, the following two versions of the MLEV-4 cycle are considered, where the cycle time of the complete *kin* sequence is given by $\tau_c = 4\tau_R$. In the first version, the sequences $P_I = R_I\bar{R}_I\bar{R}_IR_I$ and $P_S = R_S\bar{R}_S\bar{R}_SR_S$ are applied simultaneously to spins I and S. The bars represent overall phase shifts of the composite pulses by 180°. In this case, the angle $\Delta\alpha(t)$ for $0 \leqslant t \leqslant \tau_c$ is completely determined by the angle $\Delta\alpha(t)$ during the interval $0 \leqslant t \leqslant \tau_R = \tau_c/4$:

$$\Delta\alpha(t) = \begin{cases} \Delta\alpha(t) & \text{for } 0 \leqslant t < \tau_R \\ \Delta\alpha(\tau_R) - \Delta\alpha(t - \tau_R) & \text{for } \tau_R \leqslant t < 2\tau_R \\ -\Delta\alpha(t - 2\tau_R) & \text{for } 2\tau_R \leqslant t < 3\tau_R \\ -\Delta\alpha(\tau_R) - \Delta\alpha(t - 3\tau_R) & \\ & \text{for } 3\tau_R \leqslant t \leqslant 4\tau_R = \tau_c. \end{cases} \quad [20]$$

This results in

$$\bar{c}_{\Delta\alpha} = \lambda_{kin} \quad [21]$$

and

$$\bar{s}_{\Delta\alpha} = 0 \quad [22]$$

with

$$\lambda_{kin} = \cos\frac{\Delta\alpha(\tau_R)}{2}\left\{\bar{c}^R_{\Delta\alpha}\cos\frac{\Delta\alpha(\tau_R)}{2} + \bar{s}^R_{\Delta\alpha}\sin\frac{\Delta\alpha(\tau_R)}{2}\right\}, \quad [23]$$

$$\bar{c}^R_{\Delta\alpha} = \frac{1}{\tau_R}\int_0^{\tau_R} \cos\,\Delta\alpha(t)dt, \quad [24]$$

$$\bar{s}^R_{\Delta\alpha} = \frac{1}{\tau_R}\int_0^{\tau_R} \sin\,\Delta\alpha(t)dt. \quad [25]$$

In the second version of the MLEV-4 cycle, the sequences $P'_I = R_IR_I\bar{R}_I\bar{R}_I$ and $P'_S = R_SR_S\bar{R}_S\bar{R}_S$ are applied simultaneously to spins I and S and the angle $\Delta\alpha'(t)$ is given by

$$\Delta\alpha'(t) = \begin{cases} \Delta\alpha(t) & \text{for } 0 \leqslant t < \tau_R \\ \Delta\alpha(\tau_R) + \Delta\alpha(t - \tau_R) & \text{for } \tau_R \leqslant t < 2\tau_R \\ 2\Delta\alpha(\tau_R) - \Delta\alpha(t - 2\tau_R) & \text{for } 2\tau_R \leqslant t < 3\tau_R \\ \Delta\alpha(\tau_R) - \Delta\alpha(t - 3\tau_R) & \text{for } 3\tau_R \leqslant t \leqslant 4\tau_R = \tau_c \end{cases} \quad [26]$$

which results in

$$\bar{c}'_{\Delta\alpha} = \lambda_{kin}\cos[\Delta\alpha(\tau_R)] \quad [27]$$

and

$$\bar{s}'_{\Delta\alpha} = \lambda_{kin}\sin[\Delta\alpha(\tau_R)]. \quad [28]$$

Hence, both versions of the MLEV-4 cycle create an average Hamiltonian of the desired form of $\mathcal{H}_{\text{ideal}}$ (Eq. [1]) with an effective coupling constant $J_{IS}^{\text{eff}} = \lambda_{kin}\bar{J}_{IS,twin} \leqslant \lambda_{kin}J_{IS}/2$. The scaling factor $\lambda_{kin}$ (Eq. [23]) depends only on the angle $\Delta\alpha(t)$ during the duration $\tau_R$ of a single composite pulse.

## SEQUENCE DEVELOPMENT

Novel *kin* sequences were developed for a range of relative bandwidths $\Delta\nu_I/\Delta\nu_S$ with the help of an extended ver-

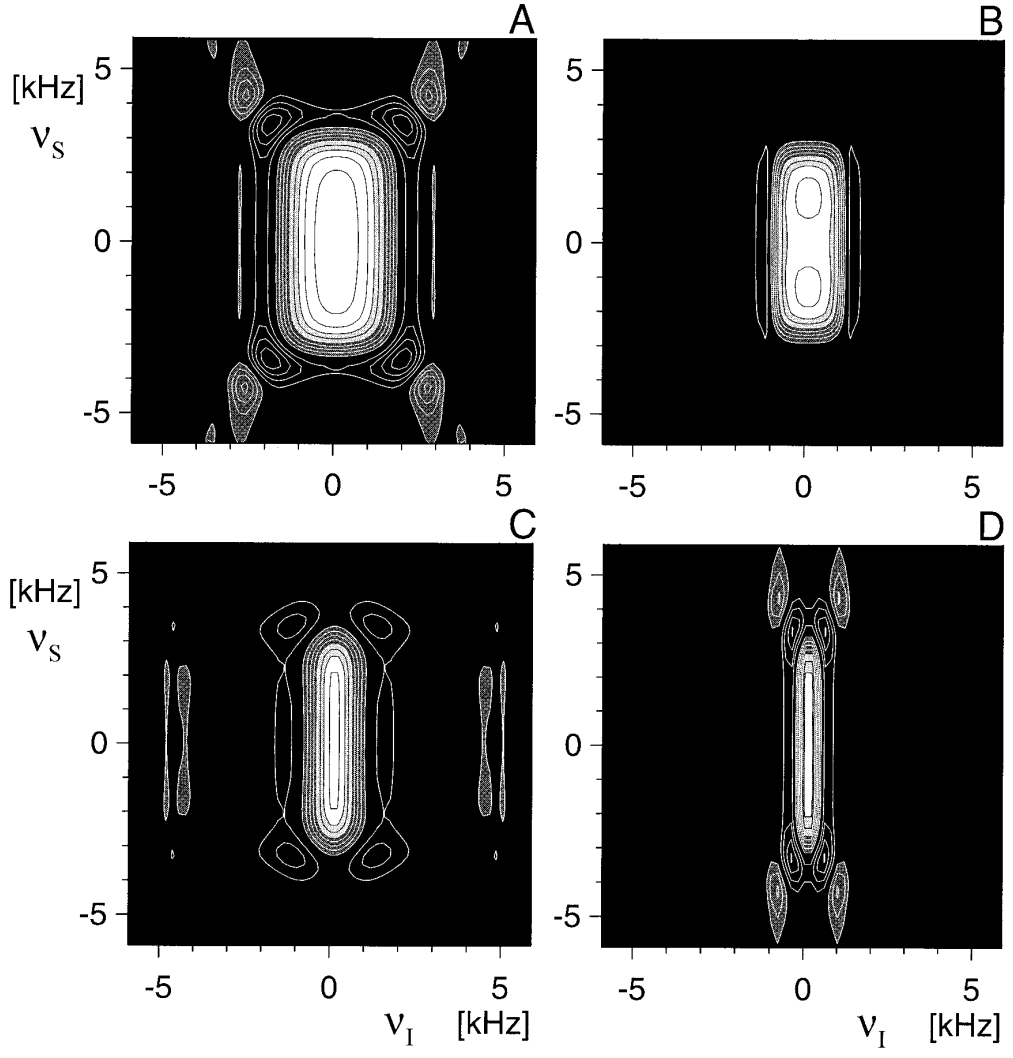


**FIG. 2.** For $J_{IS} = 90$ Hz, the simulated polarization-transfer amplitude $T_{IS,sim}(\tau)$ is shown at $\tau = 1/J_{IS}$ as a function of the offsets $\nu_I$ and $\nu_S$ in the range of ±6 kHz for the TC-2 (A), TC-3 (B), TC-5 (C), and TC-10 (D) ''*kin*'' HEHAHA sequences in the presence of RF inhomogeneity. An uncorrelated Gaussian RF-field distribution with a full width at half-height of 10% of the nominal RF-field strength was assumed in the simulations. Offset regions with $T_{IS,sim}(\tau) < 0.1$ are colored black, regions with $0.1 < T_{IS,sim}(\tau) < 0.5$ are dark gray, regions with $0.5 < T_{IS,sim}(\tau) < 0.7$ are light gray, and regions with $0.7 < T_{IS,sim}(\tau) < 1.0$ are white. The contour level spacing is 0.1.

sion of the program SIMONE (*21, 26*). In the optimizations, both composite pulses $R_I$ and $R_S$ consisted of five phase-alternated square pulses with constant RF amplitudes $\nu_1$. No restriction was imposed on the overall flip angles of $R_I$ and $R_S$. The RF amplitude $\nu_1$ was equal for both nuclei, but was allowed to vary between 4.5 and 8.5 kHz during the optimization procedure. In contrast to *twin* HEHAHA sequences, where the ratio $\Delta\nu_I/\Delta\nu_S$ of the active bandwidths is always 1, this condition does not apply to *kin* sequences and four searches were performed to find sequences with $\Delta\nu_I/\Delta\nu_S$ ratios of 1/2, 1/3, 1/5, and 1/10, respectively. More specifically, the target active bandwidth $\Delta\nu_I$ of spin I was set to 2, 1.33, 0.8, and 0.4 kHz, whereas the target bandwidth $\Delta\nu_S$ = 4 kHz of spin S was kept constant.

A hierarchical search and optimization procedure was used (*5, 26*). The first level of optimization was based on local quality factors (*5, 21, 26, 27*) that reflect the efficiency of coherence transfer in the absence of experimental imperfections. In order to find robust sequences for practical applications, experimental RF inhomogeneity was taken into account in the second level of optimization. As in practice usually two different RF coils are used to create the RF fields at the resonance frequencies of the two spin species I and S, the coherence-transfer properties were checked in the presence of an uncorrelated Gaussian RF field distribution with a width of 10% (*21*).

For each search, two offset regions were considered. Region A, where efficient Hartmann–Hahn transfer between spins I and S was desired, comprised spin pairs with offsets

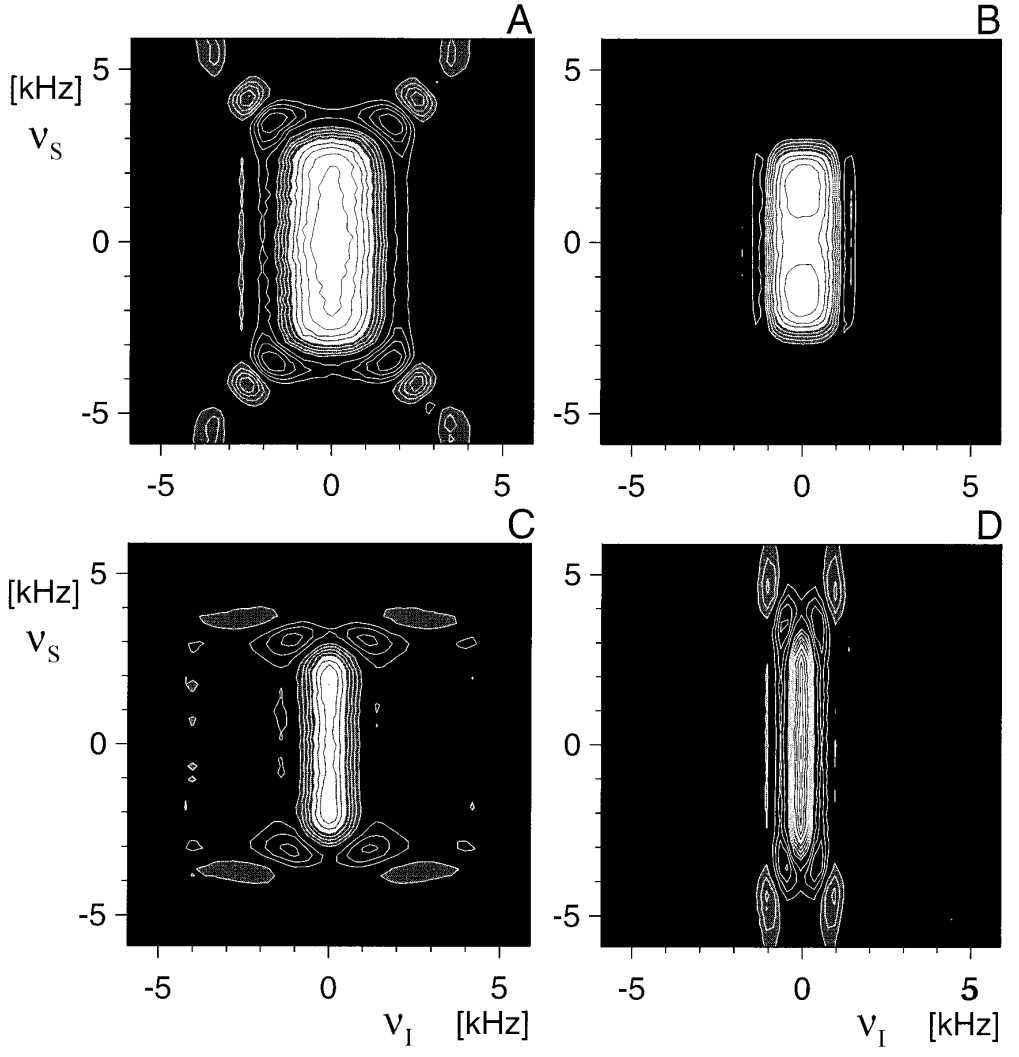


**FIG. 3.** Experimental polarization-transfer amplitude $T_{IS,exp}(\tau)$ at $\tau \approx 1/J_{IS}$ shown as a function of the offsets $\nu_I$ and $\nu_S$ in the range of ±6 kHz for the TC-2 (A), TC-3 (B), TC-5 (C), and TC-10 (D) sequences. For TC-2, TC-3, TC-5, and TC-10 sequences, eight, six, eight, and seven complete MLEV-4 cycles were used, corresponding to $\tau$ = 11.76, 11.46, 11.04, and 12.04 ms, respectively. In the experiments, the spins I and S are represented by $^1$H and $^{15}$N spins of labeled *N*-Boc-alanine in DMSO. Offset regions with $T_{IS,exp}(\tau) < 0.1$ are colored black, regions with $0.1 < T_{IS,exp}(\tau) < 0.5$ are dark gray, regions with $0.5 < T_{IS,exp}(\tau) < 0.7$ are light gray, and regions with $0.7 < T_{IS,exp}(\tau) < 1.0$ are white. The contour level spacing is 0.1.

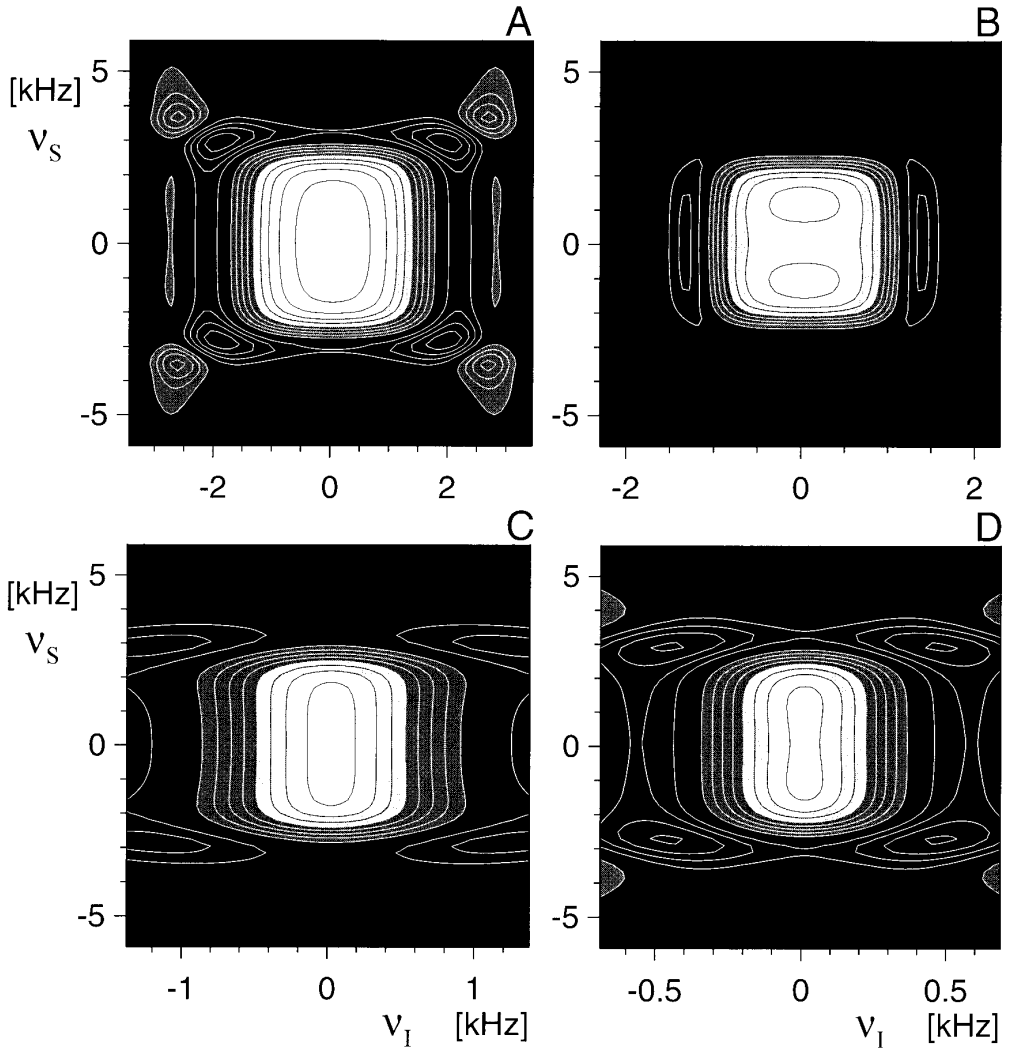


**FIG. 4.** As in Fig. 2, the simulated polarization-transfer amplitude $T_{IS,sim}(\tau)$ at $\tau = 1/J_{IS}$ is shown for $J_{IS} = 90$ Hz. In the $\nu_I$ dimension, the resolution is increased by reducing the offset ranges $\nu_I$ to $\pm 6$ kHz/2 = $\pm 3$ kHz, $\pm 6$ kHz/3 = $\pm 2$ kHz, $\pm 6$ kHz/5 = $\pm 1.2$ kHz, and $\pm 6$ kHz/10 = $\pm 0.6$ kHz for TC-2 (A), TC-3 (B), TC-5 (C), and TC-10 (D), respectively.

$\nu_I$ and $\nu_S$ in the range of $-0.5\ \Delta\nu_I \leqslant \nu_I \leqslant 0.5\ \Delta\nu_I$ and $-2$ kHz $\leqslant \nu_S \leqslant 2$ kHz. Region B, where heteronuclear Hartmann–Hahn transfer was undesired, consisted of four subregions which comprised spin pairs with offsets in the range of $-0.5\ \Delta\nu_I \leqslant \nu_I \leqslant 0.5\ \Delta\nu_I$ and 3 kHz $\leqslant \nu_S \leqslant 5$ kHz or $-3$ kHz $\leqslant \nu_S \leqslant -5$ kHz, and in the range of $0.75\ \Delta\nu_I \leqslant \nu_I \leqslant 6$ kHz or $-0.75\ \Delta\nu_I \leqslant \nu_I \leqslant -6$ kHz and $-2$ kHz $\leqslant \nu_S \leqslant 2$ kHz. In the optimizations, a heteronuclear coupling constant $J_{IS} = 90$ Hz was assumed, which is characteristic for $^1J(^1\mathrm{H}, ^{15}\mathrm{N})$ couplings.

## RESULTS

Table 1 summarizes the parameters of the new *kin* HEHAHA sequences termed TC-2, TC-3, TC-5, and TC-10 with $\Delta\nu_I/\Delta\nu_S$ ratios of 1/2, 1/3, 1/5, and 1/10, respectively. The basic composite pulses $R_I$ and $R_S$ of these sequences are shown in Figs. 1A–1D. As the sequence elements $R_I$ and $R_S$ approach composite 180° pulses, the effective fields $B_I^{eff}$ and $B_S^{eff}$ created by the MLEV-4 expanded sequences $P_I$ and $P_S$ approach zero if spins I and S are irradiated close to resonance (*25*); i.e., the Hartmann–Hahn condition $\gamma_I B_I^{eff} = \gamma_S B_S^{eff}$ is fulfilled. As shown in Fig. 1, for all sequences, we find $\Delta\alpha(\tau_R) \approx n\ 360°$ with integer $n$. This is a prerequisite for a minimal reduction of the effective coupling constant, as according to Eq. [23], $\lambda_{kin}$ is scaled with $\cos[\Delta\alpha(\tau_R)/2]$. Furthermore, for $0 \leqslant t \leqslant \tau_R$, the angles $\Delta\alpha(t)$ are usually close to integer multiples of 360° where $\cos[\Delta\alpha(t)] \approx 1$, which leads to $\bar{c}^R_{\Delta\alpha} \approx 1$ (Eq. [24]). These

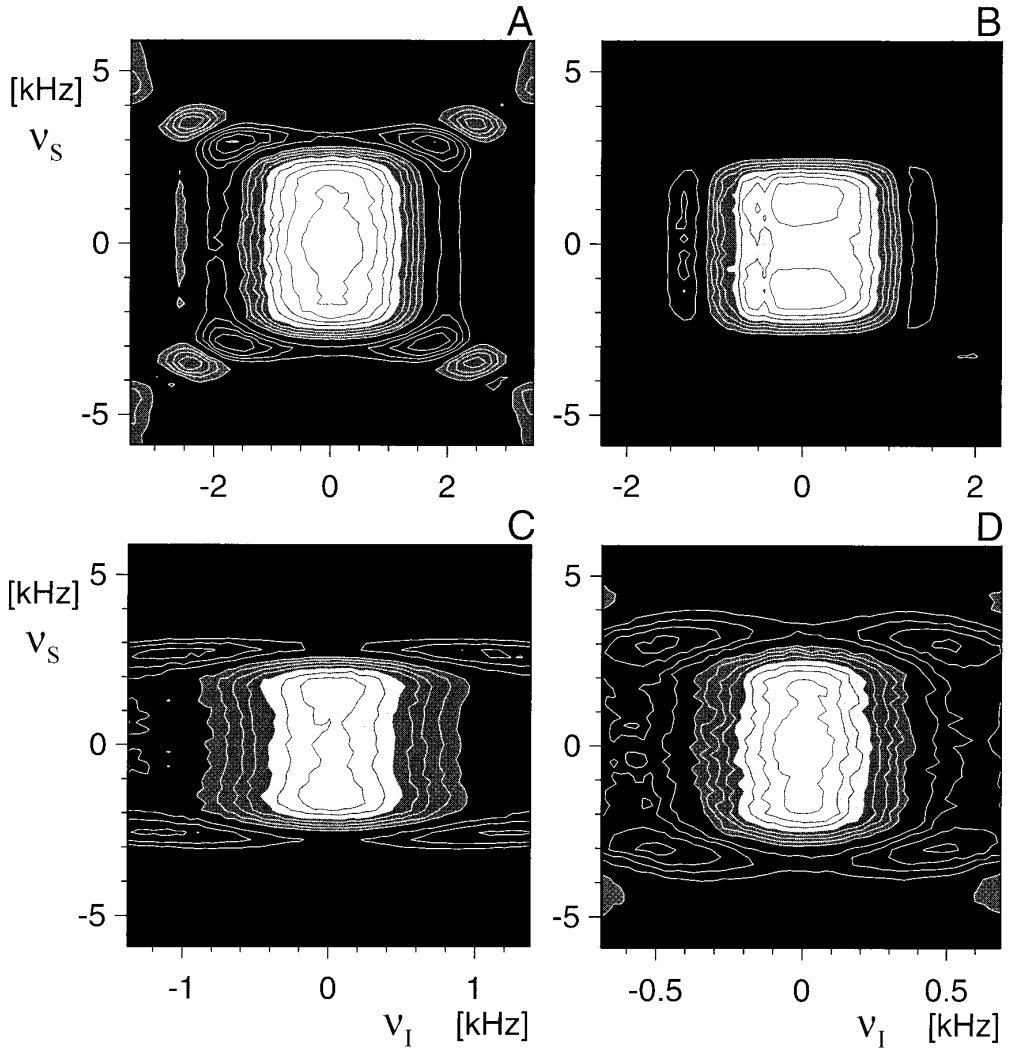


**FIG. 5.** As in Fig. 3, the experimentally determined polarization-transfer amplitude $T_{IS,sim}(\tau)$ is shown. In the $\nu_I$ dimension, the resolution is increased by reducing the offset ranges $\nu_I$ to $\pm 6$ kHz/2 = $\pm 3$ kHz, $\pm 6$ kHz/3 = $\pm 2$ kHz, $\pm 6$ kHz/5 = $\pm 1.2$ kHz, and $\pm 6$ kHz/10 = $\pm 0.6$ kHz for TC-2 (A), TC-3 (B), TC-5 (C), and TC-10 (D), respectively.

properties lead to minimal reductions of the effective coupling constants with $\lambda_{kin}$(TC-2) = 0.91, $\lambda_{kin}$(TC-3) = 0.70, $\lambda_{kin}$(TC-5) = 0.78, and $\lambda_{kin}$(TC-10) = 0.74 (cf. Eq. [23]).

The theoretical and experimental offset dependences of the HEHAHA transfer efficiency of these *kin* sequences are shown in Figs. 2 and 3 for offsets $\nu_I$ and $\nu_S$ in the range of $\pm 6$ kHz. In Figs. 4 and 5, expanded theoretical and experimental offset profiles are shown for reduced offset ranges $\nu_I$ of $\pm 6$ kHz/2 = $\pm 3$ kHz, $\pm 6$ kHz/3 = $\pm 2$ kHz, $\pm 6$ kHz/5 = $\pm 1.2$ kHz, and $\pm 6$ kHz/10 = $\pm 0.6$ kHz for TC-2, TC-3, TC-5, and TC-10, respectively.

In the theoretical offset profiles of Figs. 2 and 4, the calculated transfer amplitude of *x* magnetization is shown at the mixing time $\tau = 1/J_{IS}$ which is optimal for ideal heteronuclear planar mixing experiments (*4, 5*). For the two RF channels, an uncorrelated Gaussian RF-field distribution with a full width at half-height of 10% of the nominal RF amplitude $\nu_1$ was assumed in the simulations.

At $\tau = 1/J_{IS}$, the maximum theoretical transfer amplitudes are 97, 82, 82, and 82% for TC-2, TC-3, TC-5, and TC-10, respectively. These maximum amplitudes reflect the slight reduction of the effective coupling constants in the effective Hamiltonians. With the parameters $\Delta\alpha(\tau_R)$, $\bar{c}^R_{\Delta\alpha}$, and $\bar{s}^R_{\Delta\alpha}$, the *kin* scaling factors $\lambda_{kin}$ can be determined for each sequence (Eq. [23]) and are summarized in Table 1. According to the results derived under Theory (Eqs. [17], [24], and [25]), the MLEV-4 expanded TC sequences are expected to yield an average Hamiltonian of the form of $\mathcal{H}_{ideal}$ (Eq. [1]) with a maximum effective coupling constant $J^{eff}_{IS}$

**TABLE 2**
**Comparison of Average and Effective Hamiltonians**

| RF sequence | Cycle | $a_{yy}$ | $a_{zz}$ | $a_{zy}$ | $a_{yz}$ |
|---|---|---|---|---|---|
| TC-2 | *a* | 0.46 (0.46) | 0.45 (0.46) | 0.02 (0.00) | −0.02 (0.00) |
| | *b* | 0.44 (0.44) | 0.43 (0.44) | 0.13 (0.13) | −0.12 (−0.13) |
| TC-3 | *a* | 0.34 (0.35) | 0.36 (0.35) | 0.03 (0.00) | −0.03 (0.00) |
| | *b* | 0.29 (0.30) | 0.31 (0.30) | −0.19 (−0.18) | 0.18 (0.18) |
| TC-5 | *a* | 0.35 (0.39) | 0.43 (0.39) | 0.00 (0.00) | 0.00 (0.00) |
| | *b* | 0.34 (0.37) | 0.40 (0.37) | −0.09 (−0.13) | 0.16 (0.13 |
| TC-10 | *a* | 0.33 (0.37) | 0.42 (0.37) | 0.00 (0.00) | 0.00 (0.00) |
| | *b* | 0.28 (0.27) | 0.27 (0.27) | 0.21 (0.26) | −0.30 (−0.26) |

*Note.* The table summarizes the coefficients $a_{yy}$, $a_{zz}$, $a_{zy}$, and $a_{yz}$ of the numerically determined effective Hamiltonian of the form $\mathcal{H}_{\text{eff}} = 2\pi J_{\text{IS}}(a_{yy}I_yS_y + a_{zz}I_zS_z + a_{zy}I_yS_z + a_{yz}I_zS_y)$ for on-resonance irradiation of the spins I and S. The corresponding coefficients of the average Hamiltonian $\bar{\bar{\mathcal{H}}}'_{\text{p}}$ derived from Eq. [17] are given in parentheses. Cycle *a* corresponds to the MLEV-4 expansion $R_{\text{I}}\bar{R}_{\text{I}}\bar{R}_{\text{I}}R_{\text{I}}$ and $R_{\text{S}}\bar{R}_{\text{S}}\bar{R}_{\text{S}}R_{\text{S}}$ of the basic composite pulses, whereas cycle *b* corresponds to the expansion $R_{\text{I}}R_{\text{I}}\bar{R}_{\text{I}}\bar{R}_{\text{I}}$ and $R_{\text{S}}R_{\text{S}}\bar{R}_{\text{S}}\bar{R}_{\text{S}}$.

$= \lambda_{kin}J_{\text{IS}}/2$, provided that the *twin* sequences defined by $\mathcal{H}_{\text{RF},\Sigma}$ (Eq. [5]) create a planar average Hamiltonian $\mathcal{H}_{\text{P}}$ (cf. Eq. [13]). This condition is approximately fulfilled and the match between the predicted average Hamiltonians $\bar{\bar{\mathcal{H}}}'_{\text{P}}$ and the numerically determined effective Hamiltonians $\mathcal{H}_{\text{eff}}$ (*5, 19*) is excellent (see Table 2). As expected, the first version of the MLEV-4 cycle creates a zero-quantum angle $\phi = 0$ and the second version of the MLEV-4 cycle creates zero-quantum angles $\phi = \Delta\alpha(\tau_{\text{R}})$ (cf. Table 1).

Experimental offset profiles for the transfer efficiency of the new *kin* HEHAHA sequences were acquired on a Bruker AMX 600 spectrometer using a sample of $^{15}$N-labeled *N*-Boc-alanine dissolved in DMSO, where the $^{15}$N–$^{1}$H transfer in the NH group was monitored (*21*). The experimental transfer amplitudes were determined for a mixing time $\tau$ of approximately $1/J(^{15}\text{N}, ^{1}\text{H}) = 11.1$ ms. The mixing times used for the TC-2, TC-3, and TC-10 sequences (Figs. 3a, 3b, 3d and Figs. 5a, 5b, 5d) were slightly longer than $1/J$ because an integer number of MLEV-4 cycles was used. Therefore, the maximum experimental transfer is higher than that in the calculated offset plots. In general, the agreement between the theoretical and experimental transfer profiles is excellent.

## CONCLUSIONS

This work demonstrates that efficient magnetization transfer between two scalar-coupled heteronuclear spins is possible with *kin* HEHAHA sequences that are based on the simultaneous application of two *different* multiple-pulse sequences $P_{\text{I}}$ and $P_{\text{S}}$. With the help of *kin* HEHAHA sequences, magnetization can be selectively transfered between two different bandwidths $\Delta\nu_{\text{I}}$ and $\Delta\nu_{\text{S}}$. In addition to the selectivity of heteronuclear polarization transfer, the simultaneously occurring homonuclear Hartmann–Hahn transfer (*4, 5, 16, 28, 29*) between scalar-coupled I (or S) spins is also selectively restricted by the two different bandwidths $\Delta\nu_{\text{I}}$ and $\Delta\nu_{\text{S}}$, respectively. Compared to conventional *twin* HEHAHA experiments, the introduction of *kin* sequences markedly increases the flexibility of HEHAHA experiments. The new sequences TC-2, TC-3, TC-5, and TC-10 achieve bandwidth ratios $\Delta\nu_{\text{I}}/\Delta\nu_{\text{S}}$ of up to 1/10 with a reduction of the effective coupling constant by less than 30% compared to an ideal planar HEHAHA experiment. If the mixing time $\tau_{\text{mix}} = 1/J_{\text{IS}}$ is correspondingly increased, complete polarization transfer can be achieved in the absence of relaxation. Although this paper is focused on *heteronuclear kin*-type Hartmann–Hahn sequences, applications to doubly band-selective *homonuclear* Hartmann–Hahn experiments (*9, 30–32*) are also possible. Furthermore, the use of *kin*-type sequences is not restricted to *planar* mixing experiments, but can also be developed for heteronuclear or doubly band-selective homonuclear *isotropic* mixing experiments (*5, 33–35*).

## ACKNOWLEDGMENTS

This work was supported by the DFG under Grant Gl 203/1-3 and Gl 203/1-5. T.C. acknowledges a Short-Term Fellowship by the EMBO and thanks the Italian MURST for support. B.L. acknowledges a scholarship of the Fonds der Chemischen Industrie. S.J.G. thanks the DFG for a Heisenberg Stipendium (Gl 203/2-1).

## REFERENCES

1. S. R. Hartmann and E. L. Hahn, *Phys. Rev.* **128,** 2042 (1962).
2. L. Müller and R. R. Ernst, *Mol. Phys.* **38,** 963 (1979).
3. G. C. Chingas, A. N. Garroway, R. D. Bertrand, and W. B. Moniz, *J. Chem. Phys.* **74,** 127 (1981).
4. M. Ernst, C. Griesinger, R. R. Ernst, and W. Bermel, *Mol. Phys.* **74,** 219 (1991).

5. S. J. Glaser and J. J. Quant, *in* ''Advances in Magnetic and Optical Resonance'' (W. S. Warren, Ed.), Vol. 19, p. 59, Academic Press, San Diego, 1996.
6. A. Majumdar and E. R. P. Zuiderweg, *J. Magn. Reson. B* **133,** 19 (1995).
7. V. V. Krishnan and M. Rance, *J. Magn. Reson. A* **116,** 97 (1995).
8. W. R. Croasmun and R. M. K. Carlson (Eds.), ''Two-Dimensional NMR Spectroscopy: Applications for Chemists and Biochemists,'' VCH Publishers, New York, 1994.
9. T. Carlomagno, M. Maurer, M. Sattler, M. G. Schwendinger, S. J. Glaser, and C. Griesinger, *J. Biomol. NMR* **8,** 161 (1996).
10. G. W. Kellogg, A. A. Szewczak, and P. B. Moore, *J. Am. Chem. Soc.* **114,** 2727 (1992).
11. G. W. Kellogg and B. I. Schweitzer, *J. Biomol. NMR* **3,** 577 (1993).
12. U. Haeberlen, *in* ''Advances in Magnetic Resonance'' (J. S. Waugh, Ed.), Suppl. 1, p. 1, Academic Press, San Diego, 1976.
13. R. R. Ernst, G. Bodenhausen, and A. Wokaun, ''Principles of Nuclear Magnetic Resonance in One and Two Dimensions,'' Clarendon Press, Oxford, 1987.
14. D. W. Bearden and L. R. Brown, *Chem. Phys. Lett.* **163,** 432 (1989).
15. D. Canet, P. Tekely, K. Elbayed, and F. Humbert, *Chem. Phys. Lett.* **175,** 343 (1990).
16. L. R. Brown and B. C. Sanctuary, *J. Magn. Reson.* **91,** 413 (1991).
17. D. Yu. Artemov, *J. Magn. Reson.* **91,** 405 (1991).
18. J. S. Waugh, *J. Magn. Reson.* **50,** 30 (1982).
19. J. S. Waugh, *J. Magn. Reson.* **68,** 189 (1986).
20. N. Sunitha Bai, N. Hari, and R. Ramachandran, *J. Magn. Reson. A* **106,** 248 (1994).
21. M. G. Schwendinger, J. Quant, S. J. Glaser, and C. Griesinger, *J. Magn. Reson. B* **111,** 115 (1994).
22. M. Kadkhodaei, O. Rivas, M. Tan, A. Mohebbi, and A. J. Shaka, *J. Magn. Reson.* **91,** 437 (1991).
23. F. J. Dyson, *Phys. Rev.* **75,** 486, 1736 (1949).
24. R. P. Feynman, *Phys. Rev.* **84,** 108 (1951).
25. M. H. Levitt, R. Freeman, and T. Frenkiel, *in* ''Advances in Magnetic Resonance'' (J. S. Waugh, Ed.), Vol. 11, p. 47, Academic Press, San Diego, 1983.
26. S. J. Glaser and G. P. Drobny, *in* ''Advances in Magnetic Resonance'' (W. S. Warren, Ed.), Vol. 14, p. 35, Academic Press, San Diego, 1990.
27. S. J. Glaser, *J. Magn. Reson. A* **104,** 283 (1994).
28. J. M. Richardson, R. T. Clowes, W. Boucher, P. J. Domaille, C. H. Hardman, J. Keeler, and E. D. Laue, *J. Magn. Reson. B* **101,** 223 (1993).
29. K. H. Gardner and J. E. Coleman, *J. Biomol. NMR* **4,** 761 (1994).
30. R. Konrat, I. Burghardt, and G. Bodenhausen, *J. Am. Chem. Soc.* **113,** 9135 (1991).
31. M. Shirakawa, M. Wälchli, M. Shimizu, and Y. Kyogoku, *J. Biomol. NMR* **5,** 323 (1995).
32. E. R. P. Zuiderweg, L. Zeng, B. Brutscher, and R. C. Morshauer, *J. Biomol. NMR* **8,** 147 (1996).
33. D. P. Weitekamp, J. R. Garbow, and A. Pines, *J. Chem. Phys.* **77,** 2870 (1982).
34. P. Caravatti, L. Braunschweiler, and R. R. Ernst, *Chem. Phys. Lett.* **100,** 305 (1983).
35. J. Quant, S. J. Glaser, and C. Griesinger, 36th Experimental NMR Conference, Boston, Massachusetts, 1995.